Hybrid metamaterials combining pentamode lattices and phononic plates

A. O. Krushynska,[1,a)] P. Galich,[2] F. Bosia,[3] N. M. Pugno,[1,4,5] and S. Rudykh[6,b)]
[1]*Laboratory of Bio-Inspired and Graphene Nanomechanics, University of Trento, Trento 38123, Italy*
[2]*Department of Aerospace Engineering, Technion–Israel Institute of Technology, Haifa 32000, Israel*
[3]*Department of Physics and Nanostructured Interfaces and Surfaces Centre, University of Turin, Turin 10125, Italy*
[4]*School of Engineering and Materials Science, Queen Mary University of London, London E1 4NS, United Kingdom*
[5]*Ket Labs, Edoardo Amaldi Foundation, Italian Space Agency, Rome 00133, Italy*
[6]*Department of Mechanical Engineering, University of Wisconsin–Madison, Madison, Wisconsin 53706, USA*

(Received 14 August 2018; accepted 25 October 2018; published online 13 November 2018)

We propose a design strategy for hybrid metamaterials with alternating phononic plates and pentamode units that produce complete bandgaps for elastic waves. The wave control relies on the simultaneous activation of two scattering mechanisms in the constituent elements. The approach is illustrated by numerical results for a configuration comprising phononic plates with cross-like cavities. We report complete bandgaps of tunable width due to variations of geometric parameters. We show that the wave attenuation performance of the hybrid metamaterials can be further enhanced through implementation of lightweight multiphase material compositions. These give rise to efficient wave attenuation in challenging low-frequency regions. The proposed design strategy is not limited to the analyzed cases alone and can be applied to various designs of phononic plates with cavities, inclusions or slender elements. *Published by AIP Publishing.*
https://doi.org/10.1063/1.5052161

Phononic and acoustic metamaterials demonstrate unusual mechanical properties[1,2] and the ability to control elastic waves by producing bandgaps[3–5] or negative group velocity.[6,7] They draw these remarkable functionalities from their engineered architectures, giving rise to unconventional dynamic characteristics in various frequency ranges. Numerous two-dimensional (2D) configurations with periodic patterns have been designed to activate wave manipulation mechanisms, resulting in omnidirectional, complete bandgaps for plane-polarized elastic waves (2D bandgaps).[8] Applications of such designs to three-dimensional (3D) geometries are usually characterized by poor attenuation of oblique or normally incident waves.[8,9] Common examples are phononic plates with voids[10] or internal resonators[11–13] that can manipulate waves in the plane of a plate, while waves with out-of-plane wavevector components can propagate freely.[9,13,14] This issue substantially limits the potential of 2D metamaterials for engineering applications, including seismic wave shielding,[15,16] vibration mitigation,[3,6,13] or wave focusing and splitting.[17,18]

Here, we propose a design strategy specially aimed at extending 2D bandgaps in phononic plates to a full 3D setting. We show that hybrid metamaterials, consisting of phononic plates interlayered by pentamode lattice units, exhibit complete 3D bandgaps due to the simultaneous activation of wave scattering in the plates and the hybrid structure.

Pentamode lattices belong to a class of "extremal materials" as introduced by Milton and Cherkaev.[19–21] These essentially 3D structures consist of periodic repetitions of four tapered bars meeting at point-like joints in a diamond-like lattice. Ideal pentamodes have zero shear modulus, and thus exhibit fluid-like dynamics, inhibiting the propagation of shear waves at any frequency.[19,22,23] Realistic structures are characterized by a finite, non-zero effective shear modulus. Typically, this modulus is much smaller than the effective bulk modulus.[23,24] Shear and compressional waves are thus weakly coupled. This leads to frequency intervals with a single compressional mode. As we shall show, the hybrid structures formed by a combination of pentamode lattices and phononic plates can be designed to produce 3D bandgaps. Such metastructures enable bandgap tuning by adjusting the geometrical parameters and maintain structural integrity due to incorporated spheres at the joints.

A typical phononic plate has an essentially 2D configuration if its cross-section is invariant along the thickness. This simplifies theoretical analysis of the plate dynamics, possible optimization procedures, and manufacturing processes. A 2D formulation of the related elastodynamic problem for the cross-sectional geometry (assuming an infinite thickness of the plate) enables the decoupling of motions into in-plane modes with displacements $\{u_x, u_y\}$ and out-of-plane (or transverse) modes with displacements u_z.[8,9] Scattering mechanisms for these mode families are governed by a 2D elasticity tensor and a shear modulus, respectively. This results in 2D bandgaps at different frequencies for different mode types.[9,11] In a 3D plate of finite thickness, the separation of modes is, in general, not possible. For waves in the cross-sectional plane, the band structures of in-plane and out-of-plane modes are superimposed, while for oblique incident waves, the two mode types are coupled, leading to the closing of bandgaps (see Figs. S1–S3 in the supplementary material). In order to induce complete 3D bandgaps, one needs to introduce a wave attenuation mechanism in the out-of-plane direction, suppressing the coupled modes. This is

a)Electronic mail: akrushynska@gmail.com. URL: https://sites.google.com/site/mechmetamat
b)Electronic mail: rudykh@wisc.edu

typically done by developing a new 3D configuration from scratch, neglecting the extensive knowledge and data available for 2D designs. Our approach, in contrast, relies on preserving and using the wave attenuation abilities of 2D phononic plates in 3D hybrid metamaterials.

An example of the proposed hybrid metamaterials is a combination of phononic plates with cross-like cavities (known for their ability to induce wide 2D bandgaps[10]) interlayered by pentamode units. The metamaterial unit cell [Fig. 1(a), on the left] can be periodically repeated along the z axis to form a 1D meta-chain or populated along the three axial directions into a 3D structure. An extended face-centered-cubic lattice, typical for the pentamode, is thus replaced by a tetragonal lattice with the Brillouin zone shown in Fig. 1(b).[25] To maintain the structural stability, we introduce elastic spheres connecting the lattice bars to each other and to the plates. The center and end diameters of a bar are denoted by D and d, respectively; the radius of the connection spheres is R. The bar length is $\sqrt{3}a/4$, where a denotes the height of the pentamode element [Fig. 1(a), on the right]. The cross-like cavity is defined by length b, width c, and depth h. The unit cell dimensions are $a_1 \times a_1 \times a_3$ with $a_1 = a + 2R$ and $a_3 = a + 2h$. The examples considered here are for structures made of the isotropic titanium alloy Ti6A14V[26] with Young's modulus $E = 120\,\text{GPa}$, Poisson's ratio $\nu = 0.33$, and mass density $\rho = 4450\,\text{kg/m}^3$.

Wave dispersion is evaluated numerically in Comsol Multiphysics 5.2 by applying Bloch-Floquet boundary conditions at the three pairs of the plate faces and solving the related eigenfrequency problem for wavenumbers along the borders of the irreducible Brillouin zone [Fig. 1(b)]. Figure 2 shows the dispersion relation for the hybrid metamaterial with $a = 16\,\text{mm}$, $d = 0.2\,\text{mm}$, $D = 1.2\,\text{mm}$, $R = 0.1a$, $h = 0.2a$, $b = 0.9a_1$, and $c = 0.25a_1$. These values are chosen to provide the widest bandgaps for the transverse and in-plane modes in the pentamode lattice and the phononic plate, respectively.[10,22] The color of the bands designates the mode polarization $p = \int_V |u_z|^2 dV / \int_V (|u_x|^2 + |u_y|^2 + |u_z|^2) dV$, where V is the material volume in the unit cell. Specifically, blue indicates in-plane modes, and red indicates out-of-plane modes.

The band structure diagram in Fig. 2 exhibits a complete 3D bandgap highlighted in dark gray. For waves propagating parallel to the Oxy plane, it originates from Bragg scattering in a phononic plate of thickness $2h$ with stress-free bottom and upper faces. Such a plate has a 2D bandgap between 55.7 kHz and 96.4 kHz, indicated in gray.

To understand the band-gap formation process for waves along $\Gamma - Z$, $M - A$ and $X - R$ directions, we note that the

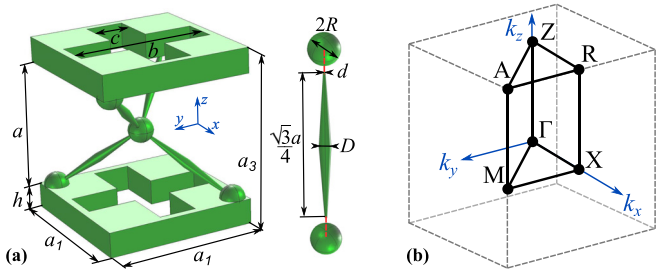

FIG. 1. (a) The unit cell of a hybrid metamaterial with cross voids and (b) irreducible Brillouin zone for a tetragonal lattice.

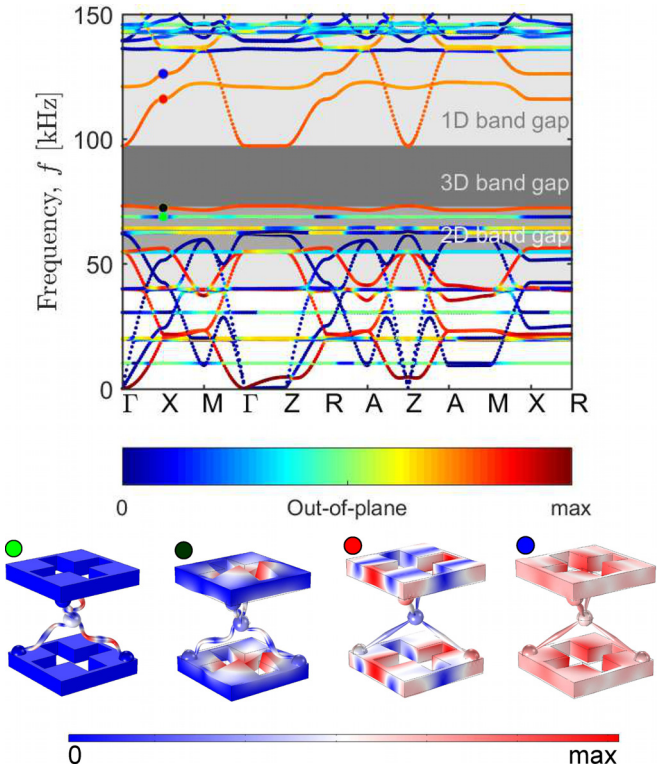

FIG. 2. Band structure for a hybrid monomaterial metastructure with cross-like voids. The color of the dispersion bands indicates the mode polarization. The colored circles refer to the vibration patterns at the selected frequencies given at the bottom.

structure of the hybrid metamaterial resembles the lattice of a zincblende crystal with tetrahedral coordination and alternating masses at lattice sites.[27] Thus, the wave propagation along the z axis can be approximated by a dispersion relation of a 1D diatomic chain (Fig. S4),[28] which is formed by two masses (a plate with half-spheres and a central sphere) connected by springs (inclined bars). The corresponding dispersion relation (see Sec. II in the supplementary material for details) is characterized by an extremely wide 1D bandgap highlighted by light gray in Fig. 2. As the real hybrid metastructure is formed by elastic plates with distributed (not lumped) masses, the vibration modes of the plates give rise to additional bands in the band structure (e.g., the mode indicated by the blue circle in Fig. 2). The Bloch-Floquet conditions at the plate boundaries also generate an additional set of modes, represented, for instance, by the localized mode marked by the green circle. As a result, the 3D bandgap has a narrow width, as compared to that of the diatomic chain, limited to the frequencies of the 2D bandgap for the plate modes. Vibration patterns at the bounds of the 3D bandgap (red and black circles) reveal strong interactions between the bars and the plates.

The introduced analogy with a diatomic chain suggests the universality of the proposed design strategy. In other words, hybrid metamaterials can be constructed for any phononic plate exhibiting 2D bandgaps (see, e.g., Fig. S6). This analogy also indicates an important role of the central sphere in the wave attenuation mechanism for the hybrid designs. On the one hand, the decrease in its mass results in the shift of the upper bandgap bound to higher frequencies. On the

other hand, the smaller the radius of the sphere, the smaller the effective axial stiffness of the bars due to the vanishing contact areas between the bars. Our simulations show that there is no bandgap for $R < 0.06a$ [Fig. S7(a)]. For larger R values, a 3D bandgap of almost constant width is induced, as the variations of the central sphere remain small compared to the mass of the plate.[29] The revealed dependence of the band-gap width on R is opposite to that for pure pentamodes, in which wide bandgaps for shear waves are obtained for vanishing contacts between the bars.[22]

Figures 3(a)–3(d) show the shapes of iso-frequency contours for the lowest out-of-plane mode (a) and (b), originating from zero frequency, and the first mode above the bandgap (c) and (d) for the two planes of the Brillouin zone [see Fig. 1(b)]. The symmetries of these contours reflect the rotation and reflection symmetries of the unit cell. For waves in the plane of the phononic plate, the hybrid metamaterial is isotropic, whereas for waves with non-zero components k_z, it is strongly anisotropic at any frequency. Similar behavior is observed for other modes (see Figs. S8 and S9).

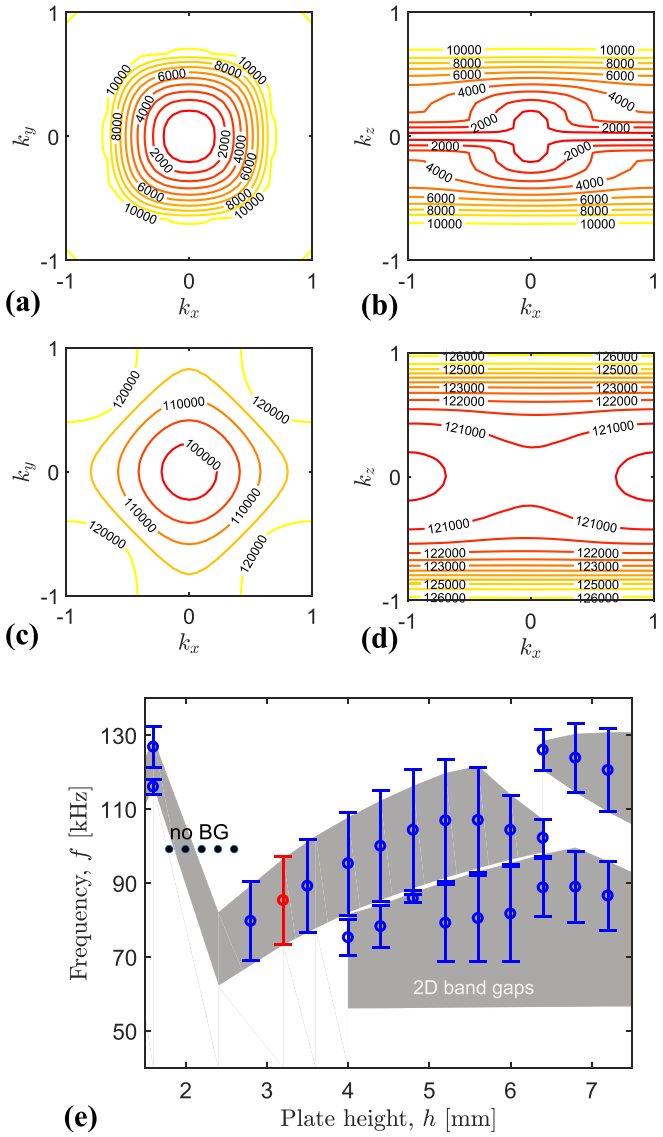

FIG. 3. (a)–(d) Directionality of plane waves propagating in Γ-*X*-*M* and Γ-*X*-*R*-*Z* planes of the Brillouin zone at low (a,b) and high (c,d) frequencies. The frequencies (in Hz) associated with the contours are labeled. (e) The bars indicate the width of 3D bandgaps for hybrid metamaterials with varying thicknesses h of the plate. The red bar corresponds to the bandgap in Fig. 2. The shaded region shows the 2D bandgaps for phononic plates of the corresponding thickness.

Next, we demonstrate that the 3D bandgap exists in a wide range of the geometric parameters, i.e., the wave-attenuation mechanisms are not limited to a particular geometric configuration of the hybrid metamaterial. Figure 3(e) presents the bandgap width versus the plate height h, with the other parameters fixed. The gray shading indicates the frequencies of the 2D bandgaps for the plates of thickness $2h$ with cross-like cavities. In most cases, the 3D bandgap occurs within the frequencies of the 2D bandgaps. However, for other parameters of the hybrid meta-structure, one can extend the 3D bandgap to slightly wider ranges (see Fig. S7). Note that by varying the plate thickness, one can tune the gap frequencies or even close the bandgap, as e.g., for $1.6 < h < 2.8$ mm. For $4 \le h \le 6$ mm, the mode marked with the black circle in Fig. 2, is shifted towards higher frequencies and separates the bandgap into two parts. As the thickness increases ($h > 6$ mm), other plate modes enter the band-gap range and split it further. Similar tunability can be achieved by varying the center diameter D of the bars [Fig. S8(b)].

We further analyze bi-material configurations with different material phases for the plate and lattice units. The key ideas here are to improve the structural integrity by decreasing the weight of the plates and to obtain more *light-weight* configurations. As an example, we consider a unit cell in Fig. 1(a) with the plates made of Nylon[30] (Young's modulus $E^{(p)} = 2$ GPa, Poisson's ratio $\nu^{(p)} = 0.41$, and mass density $\rho^{(p)} = 1200\,\mathrm{kg/m^3}$) and the pentamode bars made of titanium alloy [Fig. 4(a)]. Our simulations reveal a 3D bandgap of 22% gap width for $h = 3.5$ mm. The mid-gap frequency 22.9 kHz is about 4 times lower than that of the corresponding mono-material (titanium) configuration [Fig. 2(a)], and the effective material density $\rho^{eff} = 270\,\mathrm{kg/m^3}$ (evaluated as the sum of a material phase density multiplied by its volume fraction) is 3.3 times smaller than $\rho^{eff} = 892\,\mathrm{kg/m^3}$ for the mono-structure. Hence, apart from the improved integrity, the bi-material hybrid configuration enables the generation of 3D bandgaps in the challenging low-frequency range. This is a distinguishing feature of these designs as compared to other mass-lattice meta-structures in the literature, where low-frequency wave attenuation is achieved through the introduction of heavy masses.[5,26,30,31]

Finally, we estimate the efficiency of wave attenuation in the bi-material configurations by performing transmission analysis. The related frequency-domain finite-element simulations are performed for 5 unit-cell samples with periodic boundary conditions at the lateral faces, excited by time-harmonic normal displacements of amplitude $u_{z0} = 1\,\mu$m at one end, while the other end is attached to a perfectly matched layer (of 5 unit-cell size). For waves propagating in the $\Gamma - Z$ and $\Gamma - X$ directions [Fig. 4(b)], the curves in Figs. 4(c) and 4(d) represent the magnitude of normalized transmitted displacements $\sqrt{u_x^2 + u_y^2 + u_z^2}/u_{z0}$ averaged upon one unit cell. Elastic and damped material responses are denoted by the black and red curves, respectively. The transmission drops agree well with the bandgaps (shaded

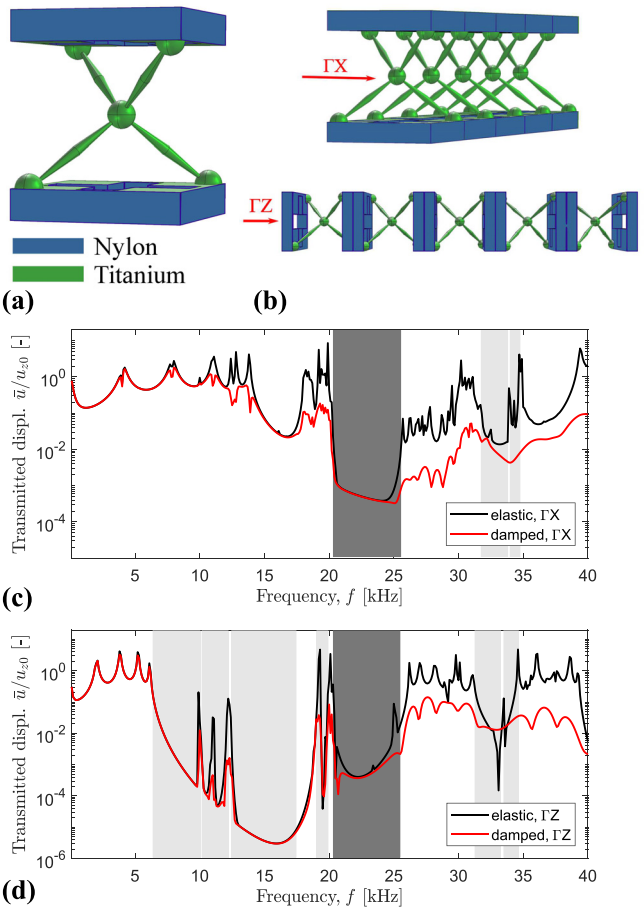

FIG. 4. (a) Unit cell of a two-phase hybrid metamaterial; (b) meta-structures composed of five unit cells. (c) and (d) Normalized transmitted displacements $\sqrt{u_x^2+u_y^2+u_z^2}/u_{z0}$ *vs.* frequency. Shaded regions indicate directional (light gray) and complete 3D (dark gray) bandgaps.

regions) or occur at frequencies of modes not excited by the applied loading [Fig. S5(b) in the supplementary material]. The small discrepancies can be attributed to the finite sizes of the samples. Note that at the frequencies of the 3D bandgap (dark gray shading), the transmission drops by three orders of magnitude, indicating excellent wave attenuation performance of the hybrid designs. The material dissipation in Nylon is implemented using a Rayleigh model with coefficients $\alpha = 1$ s^{-1} and $\beta = 4e-7$s, in agreement with the reported experimental data.[30] For titanium, we introduce the loss factor η in the stress-strain relation $\boldsymbol{\sigma} = D(1+i\eta)\boldsymbol{\epsilon}$ and assign $\eta = 0.001$ Pa s corresponding to minimum experimentally measured losses.[32] The transmission magnitude in the damped case is lower compared to the elastic case, in agreement with the predictions for lossy composites.[33,34] The amplified damping behavior at $f > 25$ kHz can be explained by the inapplicability of the Rayleigh model at these frequencies.[30]

In summary, we have proposed a design strategy for hybrid metamaterials producing 3D bandgaps for elastic waves by combining phononic plates with pentamode units. We have illustrated the idea considering an example of hybrid metamaterials considering a specific phononic plate and demonstrated the universality of the strategy for plates with various wave attenuation mechanisms. This paves the way for the development of numerous 3D metamaterials with target wave attenuation characteristics by fully exploiting the advantages of 2D configurations. For instance, one can apply powerful topology optimization techniques to design 2D geometries with required dynamic characteristics at much lower computational costs as compared to 3D cases, and then introduce them into hybrid designs with pentamode lattices by ensuring the presence of 2D bandgaps.

The proposed hybrid designs guarantee structural integrity through reinforcement of the critical joints. This becomes of importance when considering finite deformations.[35] Wave attenuation occurs for a wide range of configurations and is shown to be highly tunable by varying geometric parameters. Hence, it relies on the intrinsic structure of the proposed designs, rather than on a specific choice of geometric properties. This feature opens the way to the development of meta-structures for broadband wave attenuation by employing rainbow-type designs.[31] Moreover, we have shown that *multiphase* designs of the hybrid metastructures can further produce low-frequency attenuation characteristics in lightweight structures. The illustrative example of polymeric plates and stiff pentamodes demonstrates the potential for a broad range of engineering applications aimed at wave and vibration attenuation.

See supplementary material for 3-D band structures of phononic plates (I), details of the equivalent mass-spring model for hybrid metamaterials (II), examples for bi-material architectures (III), and geometrical variations of the design (IV).

A.K. acknowledges useful discussions with Professor C. Yilmaz from Bogazici University in Turkey. N.M.P. was supported by the European Commission with the Graphene Flagship Core 2 n. 785219 (WP14 "Composites") and FET Proactive "Neurofibres" n. 732344 as well as by the MIUR with the "Departments of Excellence" grant L. 232/2016 and ARS01-01384-PROSCAN. F.B. was supported by the EU FET Proactive "Neurofibres" Grant No. 732344 and the Progetto d'Ateneo/Fondazione San Paolo "Metapp" Project No. CSTO160004.

[1]J. Christensen, M. Kadic, O. Kraft, and M. Wegener, "Vibrant times for mechanical metamaterials," MRS Commun. **5**, 453–462 (2015).
[2]S. Cummer, J. Christensen, and A. Alu, "Controlling sound with acoustic metamaterials," Nat. Rev. Mater. **1**, 16001 (2016).
[3]S. Mohammadi, A. A. Eftekhar, A. Khelif, W. D. Hunt, and A. Adibi, "Evidence of large high frequency complete phononic band gaps in silicon phononic crystal plates," Appl. Phys. Lett. **92**, 221905 (2008).
[4]C. Crönne, E. J. S. Lee, H. Hu, and J. H. Page, "Band gaps in phononic crystals: Generation mechanisms and interaction effects," AIP Adv. **1**, 041401 (2011).
[5]L. D'Alessandro, E. Belloni, R. Ardito, F. Braghin, and A. Corigliano, "Mechanical low-frequency filter via modes separation in 3d periodic structures," Appl. Phys. Lett. **111**, 231902 (2017).
[6]M. Lee, P. Ma, I. Lee, H. Kim, and Y. Kim, "Negative refraction experiments with guided shear-horizontal waves in thin phononic crystal plates," Appl. Phys. Lett. **98**, 011909 (2011).
[7]V. Slesarenko, P. Galich, J. Li, N. Fang, and S. Rudykh, "Foreshadowing elastic instabilities by negative group velocity in soft composites," Appl. Phys. Lett. **113**, 031901 (2018).
[8]Y. Pennec, J. O. Vasseur, L. D. B. Djafari-Rouhaniand, and P. A. Deymier, "Two-dimensional phononic crystals: Examples and applications," Surf. Sci. Rep. **65**, 229–291 (2010).
[9]A. Krushynska, M. Miniaci, V. Kouznetsova, and M. Geers, "Multilayered inclusions in locally resonant metamaterials: Two-dimensional versus three-dimensional modeling," J. Vib. Acoust. **139**, 024501 (2017).

[10]Y.-F. Wang and Y.-S. Wang, "Multiple wide complete band gaps of two-dimensional phononic crystal slabs with cross-like holes," J. Sound Vib. **332**, 2019–2037 (2013).
[11]A. Krushynska, V. Kouznetsova, and M. Geers, "Towards optimal design of locally resonant acoustic metamaterials," J. Mech. Phys. Solids **71**, 179–196 (2014).
[12]P. Wang, F. Casadei, S. Shan, J. Weaver, and K. Bertoldi, "Harnessing buckling to design tunable locally resonant acoustic metamaterials," Phys. Rev. Lett. **113**, 014301 (2014).
[13]A. Krushynska, M. Miniaci, F. Bosia, and N. Pugno, "Coupling local resonance with Bragg band gaps in single-phase mechanical metamaterials," Extreme Mech. Lett. **12**, 30–36 (2017).
[14]J.-K. Huang, X.-W. Liu, X.-H. Chen, and H.-J. Xiang, "Multiple flexural-wave attenuation zones of periodic slabs with cross-like holes on an arbitrary oblique lattice: Numerical and experimental investigation," J. Sound Vib. **437**, 135–149 (2018).
[15]S. Brûlé, E. Javelaud, S. Enoch, and S. Guenneau, "Experiments on seismic metamaterials: Molding surface waves," Phys. Rev. Lett. **112**, 133901 (2014).
[16]A. Palermo, S. Krödel, K. H. Matlack, R. Zaccherini, V. K. Dertimanis, E. N. Chatzi, A. Marzani, and C. Daraio, "Hybridization of guided surface acoustic modes in unconsolidated granular media by a resonant metasurface," Phys. Rev. Appl. **9**, 054026 (2018).
[17]R. Craster and S. Gueanneau, *Acoustic Metamaterials: Negative Refraction, Imaging, Lensing and Cloaking* (Springer, Berlin, 2013).
[18]B. Liang, J.-C. Cheng, and C.-W. Qiu, "Wavefront manipulation by acoustic metasurfaces: From physics and applications," Nanophotonics **7**(6), 1191–1205 (2018).
[19]G. W. Milton and A. Cherkaev, "Which elasticity tensors are realizable?" J. Eng. Mater. Technol. **117**, 483–493 (1995).
[20]O. Sigmund, "A new class of extremal composites," J. Mech. Phys. Solids **48**, 397–428 (2000).
[21]A. Norris, "Mechanics of elastic networks," Proc. R. Soc. A **470**, 20140522 (2014).
[22]A. Martin, M. Kadic, R. Schittny, T. B. Uckmann, and M. Wegener, "Phonon band structures of three-dimensional pentamode metamaterials," Phys. Rev. B **86**, 155116 (2012).
[23]T. Bückmann, N. Stenger, M. Kadic, J. Kaschke, A. Frölich, T. Kennerknecht, C. Eberl, M. Thiel, and M. Wegener, "Tailored 3d mechanical metamaterials made by dip-in direct-laser-writing optical lithography," Adv. Mater. **24**, 2710–2714 (2012).
[24]M. Kadic, T. Bückmann, N. Stenger, M. Thiel, and M. Wegener, "On the practicability of pentamode mechanical metamaterials," Appl. Phys. Lett. **100**, 191901 (2012).
[25]R. L. Flurry, *Symmetry Groups: Theory and Chemical Applications* (Prentice-Hall, 1980).
[26]A. O. Krushynska, A. Amendola, F. Bosia, C. Daraio, N. M. Pugno, and F. Fraternali, "Accordion-like metamaterials with tunable ultra-wide low-frequency band gaps," New J. Phys. **20**, 073051 (2018).
[27]L. Kantorovich, *Quantum Theory of the Solid State: An Introduction* (Kluwer Academic Publishers, Dordrecht, 2004), p. 32.
[28]M. I. Hussein, M. Leamy, and M. Ruzzene, "Dynamics of phononics materials and structures: Historical origins, recent progress and future outlook," ASME Appl. Mech. Rev. **66**, 040802 (2014).
[29]The cases with $R > 0.1a$ are not considered here, as they require increasing the lateral plate dimensions that modifies the unit cell external sizes that prevents a fair comparison.
[30]L. D'Alessandro, E. Belloni, R. Ardito, A. Corigliano, and F. Braghin, "Modeling and experimental verification of an ulta-wide bandgap in 3d phononic crystals," Appl. Phys. Lett. **109**, 221907 (2016).
[31]S. Krödel, N. Thomé, and C. Daraio, "Modeling and experimental verification of an ultra-wide bandgap in 3d phononic crystals," Extreme Mech. Lett. **4**, 111–117 (2015).
[32]D.-G. Lee, S. Lee, and Y. Lee, "Effect of precipitates on damping capacity and mechanical properties of ti64v alloy," Mater. Sci. Eng. A **486**, 19–26 (2008).
[33]A. Krushynska, V. Kouznetsova, and M. Geers, "Visco-elastic effects on wave dispersion in three-phase acoustic metamaterials," J. Mech. Phys. Solids **96**, 29–47 (2016).
[34]V. Slesarenko and S. Rudykh, "Harnessing viscoelasticity and instabilities for tuning wavy patterns in soft layered composites," Soft Matter **12**, 3677–3682 (2016).
[35]P. Galich, N. Fang, M. Boyce, and S. Rudykh, "Elastic wave propagation in finitely deformed layered materials," J. Mech. Phys. Solids **98**, 390–410 (2017).

Hybrid Metamaterials combining Pentamode Lattices and Phononic Plates – Supplementary Materials

A.O. Krushynska,[1] P. Galich,[2] F. Bosia,[3] N.M Pugno,[1,4,5] and S. Rudykh[6]

[1)] *Laboratory of Bio-Inspired & Graphene Nanomechanics, University of Trento, Trento, Italy*[a)]

[2)] *Department of Aerospace Engineering, Technion – Israel Institute of Technology, Haifa, Israel*

[3)] *Department of Physics and Nanostructured Interfaces and Surfaces Centre, University of Turin, Turin, Italy*

[4)] *School of Engineering and Materials Science, Queen Mary University of London, London, UK*

[5)] *Ket Labs, Edoardo Amaldi Foundation, Italian Space Agency, Rome, Italy*

[6)] *Department of Mechanical Engineering, University of Wisconsin–Madison, Madison, WI, USA* [b)]

(Dated: 24 October 2018)

[a)] Electronic mail: akrushynska@gmail.com

[b)] Electronic mail: rudykh@wisc.edu

I. WAVE DISPERSION IN 3D CONFIGURATIONS OF PHONONIC PLATES

In the main part of the manuscript, we mention that phononic plates with unvarying cross-section along the thickness can manipulate plane-polarized waves, for which the out-of-plane wavevector component k_z equals to 0, and cannot control waves with non-zero waves of k_z. Here we present typical designs of such phononic plates incorporating either voids or slender elements or inclusions.

In particular, we consider a phononic plate with cross-like voids (Fig. S1a), a plate with cylindrical inclusions adjusted by slender elements to the host structure (Fig. S2a), and a phononic plate with rubber-coated heavy resonators (Fig. S3a). The geometry of the first plate (with cross-like voids) is the same as in the main text. The geometric parameters of the other two plates are optimized to induce a wide band gap.[2,3] For the plate with slender elements, these are the unit cell size of $a_1 = 25$ mm; the radius of inclusion $0.35a_1$; the radius of a cavity $0.45a_1$; the ligament thickness $0.05a_1$, and the plate thickness $0.6a_1$. The plate with coated resonators has the unit cell size $a_1 = 25$ mm, the radii of uncoated $r = 0.35a_1$ and coated $R = 0.45a_1$ inclusions, and the plate thickness $h = 0.2a_1$.

The mono-phase plates (Fig. S1a and Fig. S2a) are made of the titanium alloy described in the main text. The material phases for the plate with coated resonators are epoxy (host material) with Young's modulus $E^e = 3.6$ GPa, Poisson's ratio $\nu^e = 0.37$, and mass density $\rho^e = 1180$ kg/m^3; tungsten (resonator) with $E^t = 411$ GPa, $\nu^t = 0.28$, and $\rho^t = 19250$ kg/m^{3}3; rubber (resonator's coating) with $E^r = 150$ kPa, $\nu^r = 0.4995$, and $\rho^r = 1300$ kg/m^3.

The band structure evaluation is performed numerically by means of the Structural Modulus in Comsol Multiphysics v. 5.2. The corresponding eigenfrequency problem is solved for the wave vector values at the border of the irreducible Brillouin zone (Fig. 1b of the main text). In order to extend the plate designs to 3D configurations, we apply Floquet-Bloch periodic boundary conditions at the three pairs of faces of plate unit cells. The calculated band structure diagrams are presented in Figs. S1c-S3c, respectively. The color of the curves indicates the mode polarization. The blue color designates in-plane polarized modes with wavevector $(k_x \neq 0, k_y \neq 0, k_z = 0)$ and displacements $(u_x \neq 0, u_y \neq 0, u_z = 0)$, and the red color refers to out-of-plane modes with $(k_x \neq 0, k_y \neq 0, k_z = 0)$ and $(u_x = 0, u_y = 0, u_z \neq 0)$.[1]

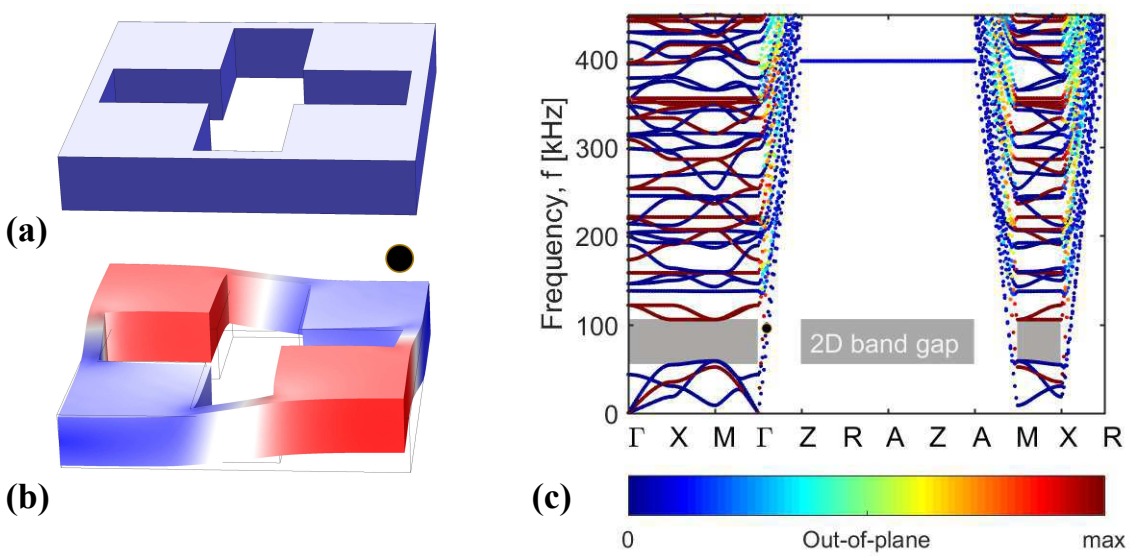

FIG. S1. (a) Unit cell of a phononic plate with a cross-like void; (b) one of the vibration patterns at the frequencies of a 2D band gap; (c) the band structure diagram, where the color of the bands indicates the mode polarization. The 2D band gaps for plane-polarized waves are shaded in gray.

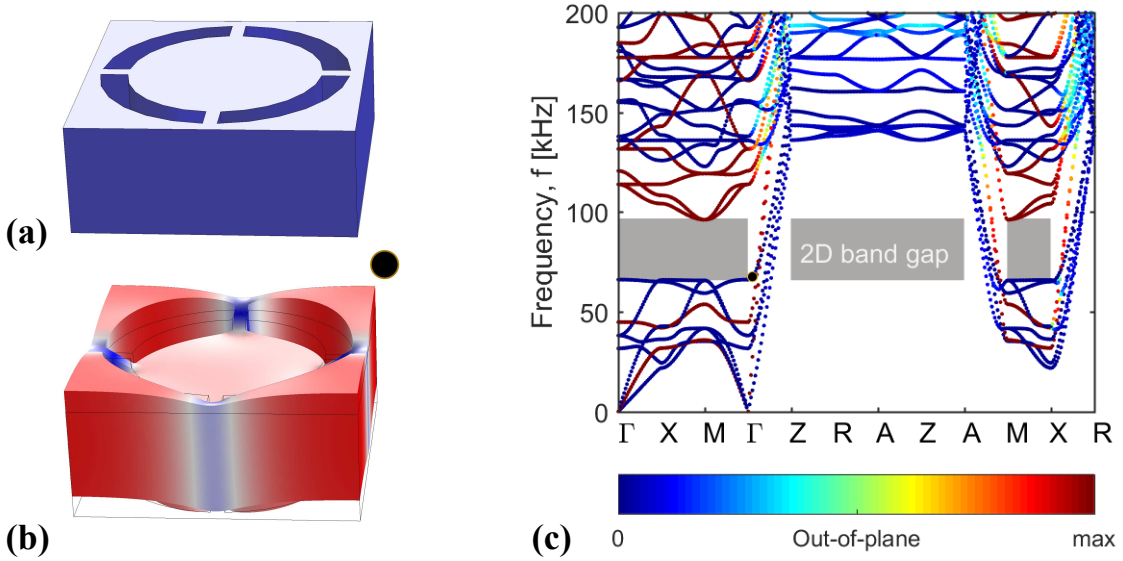

FIG. S2. (a) Unit cell of a phononic plate with slender elements; (b) one of the vibration patterns at the frequencies of a 2D band gap; (c) the band structure diagram, where the color of the bands indicates the mode polarization. The 2D band gaps for plane-polarized waves are shaded in gray.

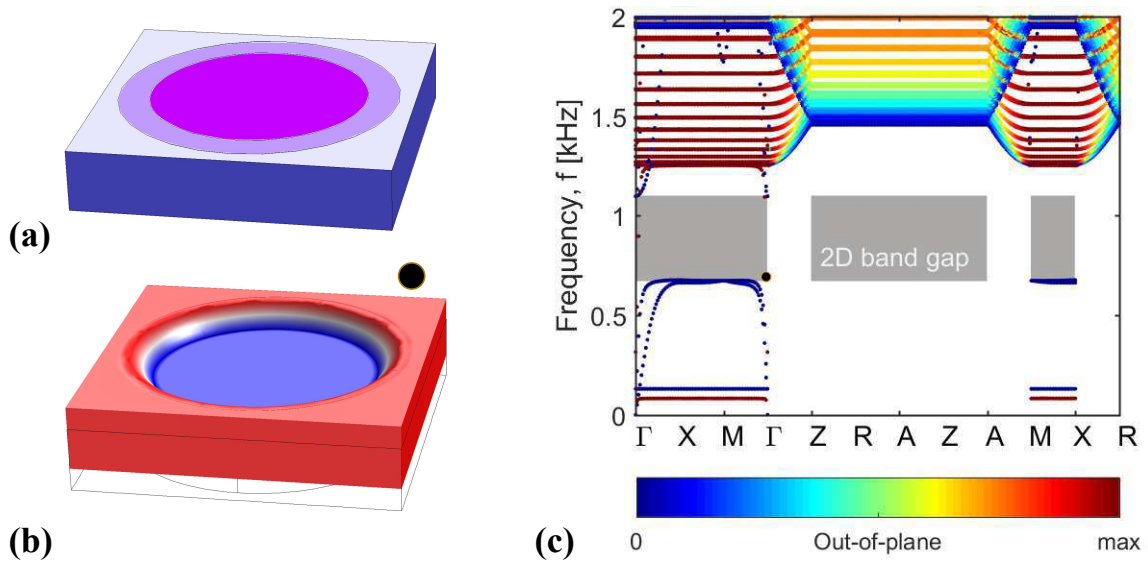

FIG. S3. (a) Unit cell of a phononic plate with coated resonators; (b) one of the vibration patterns at the frequencies of a 2D band gap; (c) the band structure diagram with the color of the bands indicating the mode polarization. The 2D band gaps for plane-polarized waves are shaded in gray.

Note that for the wave propagation directions with $k_z = 0$ (see Fig.1b of the main text), the modes are uncoupled, i.e., they are of either in-plane or out-of-plane polarization, and the mixed modes are absent. The 2D band gaps for plane-polarized waves (with $k_z = 0$) are shaded in gray. The plates with cross-like voids and slender elements have 2D band gaps at 58.56-105.3 kHz and 66-96.5 kHz, respectively; and the plate with coated inclusions has a 2D band gap between 674 Hz and 1.1 kHz. For every considered phononic plate, the generation of complete 3D band gaps is prevented due to the the mode coupling. Some typical vibration patterns at the frequencies of 2D band gaps are given in Figs. S1b-S3b. (In Figs.S1-S3b, the maximum and minimum values of displacements are depicted in red and blue, respectively).

II. EQUIVALENT MASS-SPRING MODEL FOR A HYBRID METAMATERIAL

For waves propagating along the $\Gamma - Z$ direction (see Fig. 1b of the main text), the dynamics of the proposed hybrid metamaterials can be described by using an equivalent

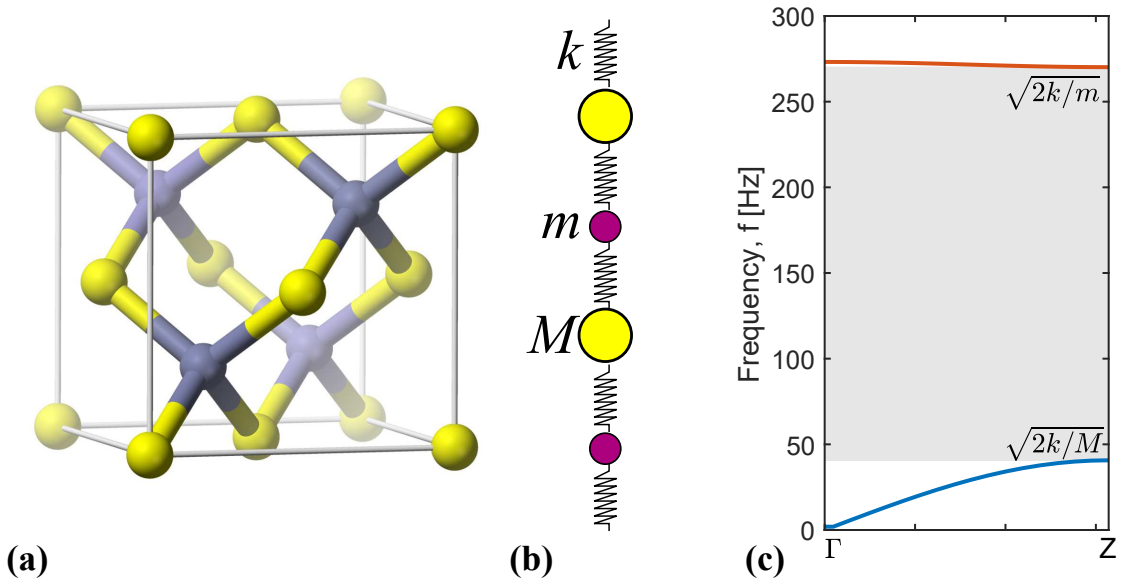

FIG. S4. (a) Zinblende unit cell (link: https://en.wikipedia.org/wiki/Cubic_crystal_system/media/File:Sphalerite-unit-cell-depth-fade-3D-balls.png). A diatomic mass-spring model (b) and the corresponding band structure (c) with 1D band gap shaded in light gray.

mass-spring model. This becomes possible since the metamaterial's structure resembles the lattice of a zincblende crystal with tetrahedral configuration and alternating masses at the lattice sites (Fig. S4a). The wave propagation along the [111] direction in such a lattice is well approximated by the dynamics of 1D diatomic mass-spring chain with the alternating masses M and m connected by identical springs of stiffness k (Fig. S4b).[4] The corresponding band structure is formed by an acoustic and an optical branches separated by a band-gap with bounding frequencies $\sqrt{2k/M}$ and $\sqrt{2k/m}$.

The effective stiffness of the inclines tapered bars forming a pentamode unit is estimated acoording to a procedure described elsewhere.[5] We consider a lower half of the hybrid metamaterial unit cell formed by a phononic plate with a cross void, two inclined bars, joint by spheres to the plane, and half of the central sphere (Fig.1a of the main text). A tensile force is distributed at the top surface of the central half-sphere, while the plate is clamped. A ratio of the applied force to an induced vertical displacement of the half-sphere provides the value of the effective stiffness of the two bars in the vertical direction $k_z^{(eff)} = 2.7858e6$ N/m. Note that up to displacements of the order of 10^{-6} m, the effective stiffness preserves its values

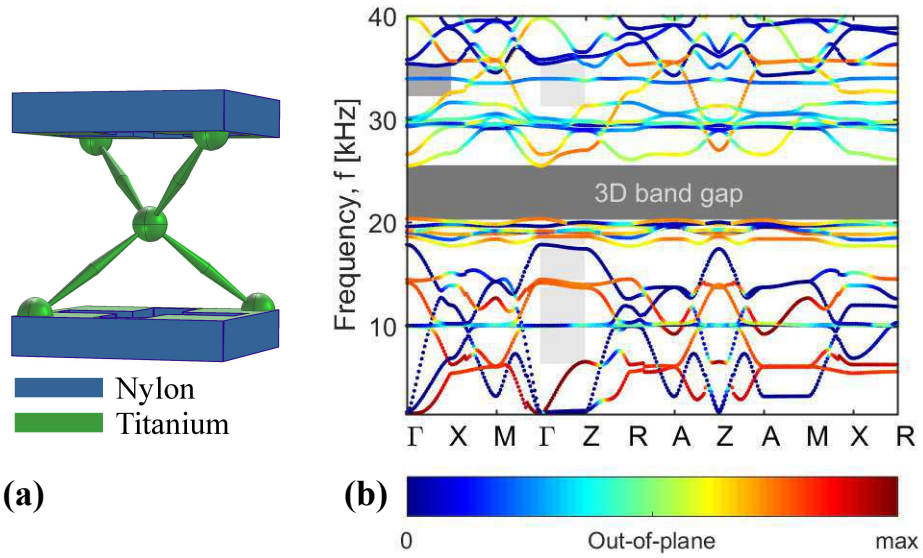

FIG. S5. Unit cell of a hybrid bi-material metastructure with cross voids (a) and the corresponding band structure diagram (b). The color of the bands indicates the mode polarization. The 3D band gap is shaded in dark gray, and the 2D band gaps for plane-polarized waves are shaded in gray.

that justifies the assumption on a linear elastic response for small-magnitude excitation. The mass m equals the mass of the central sphere in the unit cell, i.e. $m = 4/3\pi R^3\rho = 0.07635$ g, and the mass M is the sum of the mass of four half-spheres and that of a phononic plate, $M = 3.368$ g. Hence, the 1D band-gap for the equivalent mass-spring system spans the frequency range between 40.67 kHz and 270.14 kHz as shown in Fig. S4c.

III. BI-MATERIAL AND OTHER HYBRID METAMATERIAL CONFIGURATIONS

The band structure diagram for a bi-material hybrid metamaterial composed of Nylon plates with cross-like voids and titanium pentamode units (Fig. S5a) is shown in Fig. S5b. The geometric and material properties are given in the main text.

Other configurations of the hybrid metamaterials are also possible. Fig. S6a gives an example of a mono-material hybrid metastructure composed of phononic plates with slender elements.[2] The related band structure diagram is shown in Fig. S6b. The structural material is titanium alloy, and the geometric parameters for the plate and pentamode unit are the

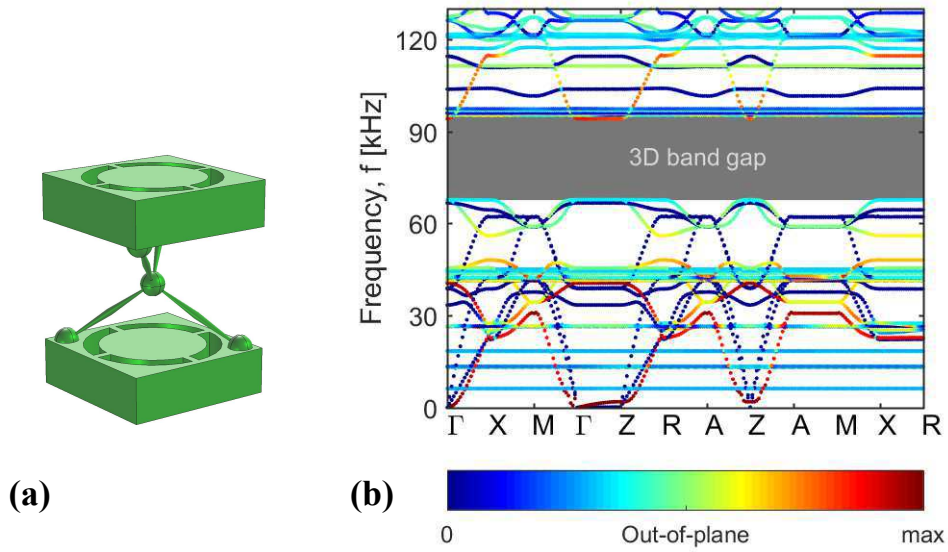

FIG. S6. (a) Unit cell of a mono-material hybrid metastructure composed of a phononic plate with slender elements and a pentamode unit. (b) The corresponding band structure diagram. The color of the bands indicates the mode polarization. The complete 3D band gap is highlighted in gray.

same as described in Section I.

IV. PARAMETRIC STUDIES

Figure S7 present the dependence of the width of a 3D band gap (shown by bars) on the radius of the joint spheres R (Fig. S7a) and the central diameter of the inclined bars D (Fig. S7b) for the mono-material hybrid configuration given in Fig. 1a of the main text. The structural material is titanium alloy, and the geometric parameters are the same as described in the main text. As can be seen, by changing the values of R or D, one can either completely close the 3D band gap or extend it to frequencies slightly higher than those of the 2D band gap for the corresponding phononic plate of thickness $2h$.

Finally, Fig. S8 presents the iso-frequency contours for the two lowest in-plane polarized modes originating from zero frequency. As can be expected, these modes are isotropic in the Oxy plane, parallel to the plate faces, and strongly anisotropic in the Oxz plane. The same behavior is observed for two modes in the higher frequency range, above the 3D band-gap frequencies (Fig. S9).

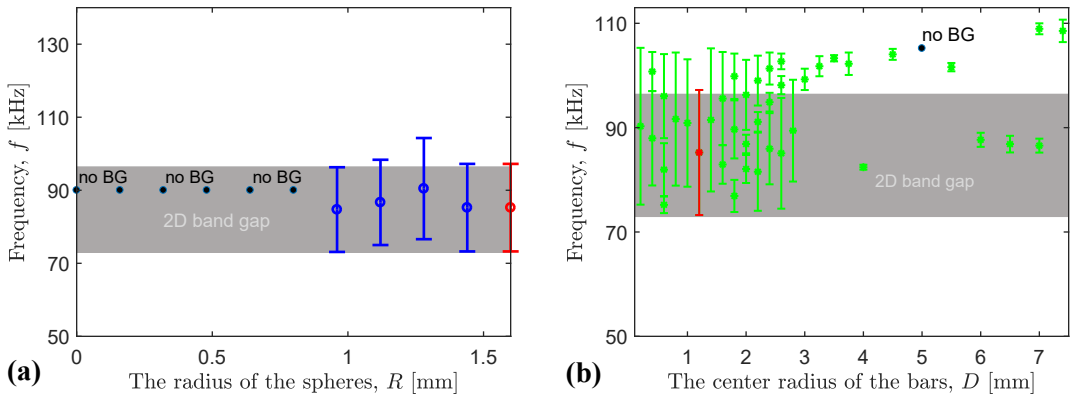

FIG. S7. The bars indicate the width of 3D band gaps for hybrid metamaterials with cross voids *vs.* (a) the radius R of the spheres at the joints and (b) the central diameter D of the lattice units. The red bar corresponds to the band gap shown in Fig. 2 of the main text. The shaded region shows the 2D band gap of a phononic plate of thickness $2h$.

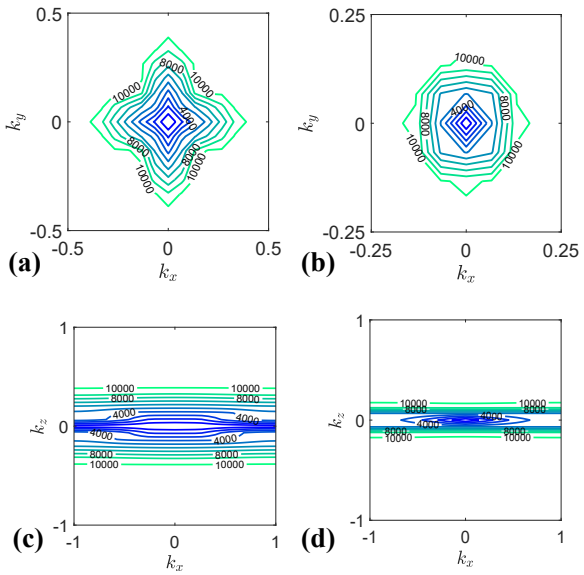

FIG. S8. Directionality of in-plane polarized waves propagating in the Oxy (a,b) and Oxz (c,d) planes of the Brillouin zone at close to zero frequencies. The frequencies (in Hz) associated with contours are labeled.

REFERENCES

[1]Pennec Y., Vasseur J.O., Djafari-Rouhaniand B., Dobrzyński L., Deymier P. A. (2010). Two-dimensional phononic crystals: Examples and applications. Surf. Sci. Rep. 65, 229—

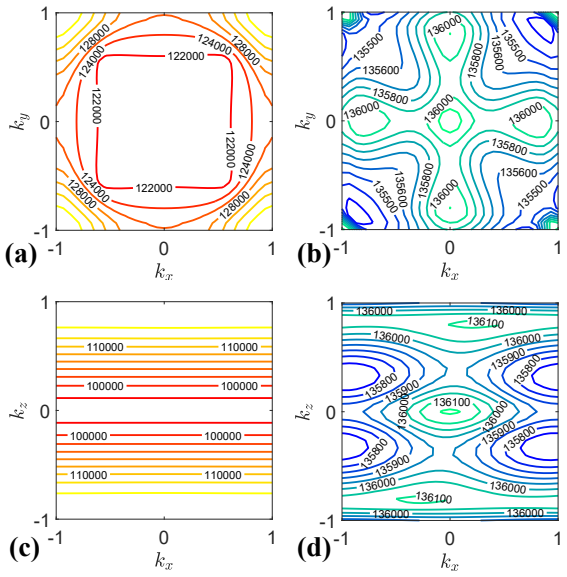

FIG. S9. Directionality of waves propagating in the Oxy (a,b) and Oxz (c,d) planes of the Brillouin zone at the frequencies above the 3D band gap. The frequencies (in Hz) associated with contours are labeled.

291.

[2]Krushynska A.O., Miniaci M., Bosia F., Pugno N.M. (2017). Coupling local resonance with Bragg band gaps in single-phase mechanical metamaterials. Extr. Mech. Lett. 12, 30-36.

[3]Krushynska A.O., Miniaci M., Kouznetsova V.G. and Geers M.G.D. (2017). Multilayered inclusions in locally resonant metamaterials: two-dimensional versus three-dimensional modeling. J. Vibr. Acoust. 139, 024501.

[4]Hussein M.I., Leamy M.J., and Ruzzene M. (2014). Dynamics of phononics materials and structures: historical origins, recent progress and future outlook. ASME Appl. Mech. Rev. 66, 040802.

[5]Krushynska A.O., Amendola A., Bosia F., Daraio C., Pugno N.M. and Fraternali F. (2018). Accordion-like metamaterials with tunable ultra-wide low-frequency band gaps. New J. Phys. 20, 073051.